Proceedings of the 16th International Conference on Soil Mechanics and Geotechnical Engineering

doi:10.3233/978-1-61499-656-9-2663

Effects of three dimensional response of dikes on their local failures during an earthquake

L'éffet de réponse tridimensionnelle de digues à leur rupture locale pendant le tremblement de terre

S. Kano & Y. Sasaki
Graduate school of Engineering, Hiroshima University, Japan
Y. Hata
Research and Development Center, Nipponkoei Co., Ltd, Japan

ABSTRACT
According to studies on seismic damage to dikes, local failures sometimes occurred during earthquakes even though foundation condition were same along the dike. The effects of three dimensional response on the local failures of dikes during earthquakes were examined by shaking table tests. The results revealed that the local failures of dikes were caused by the three dimensional response, so an equation to calculate the intervals of local failures was proposed based on three dimensional vibration equation.

RÉSUMÉ
D'après les cas des dégât de digues causés par la séisme, des ruptures locales de digues ont été constatées bien que le fond de digues ait eu des impacts de l'onde séisme uniformément. Dans ce document, on a examiné l'effet de réponse tridimentionnelle de digues à leur rupture locale pendant le tremblement de terre en faisant des expériences à l'aide de table vibrante. Des résultats acquis révèlent que la rupture locale de digues est causée par la réponse tridimentionnelle, et on propose ici, une équation afin de calculer la période des ruptures locales basée sur l'équation de la vibration avec cisaillement.

1 INTRODUCTION

Seismic damage to embankments has been sometimes found to take place at locally limited spot even though the foundation condition is almost the same along their axis.

A typical example of this type of damage was seen at the Kushiro River dike during the Kushiro-Oki Earthquake (Mj=7.8) in 1993. Table 1 shows the earthquake magnitude and the peak ground acceleration during the earthquake (Hokkaido Development Bureau, 1994). The epicenter was located about 17 km off the coast of the Kushiro city. The Kushiro River dike which had been constructed on soft ground in the Kushiro marsh was severely damaged periodically along its axis as shown in Figure 1. The reason of this periodical appearance of damaged section was not known.

The Kushiro River runs through the Kushiro marsh (203.66 km^2) and reaches to the Pacific Ocean in the Kushiro city. The dike in the Kushiro marsh had been constructed by using sandy materials on flat soft deposit. The ground surface was covered by peat layer underlain by strata of sand and clay layers.

Totally 2300 m long sections among the 3200 m long section on the left side bank in the marsh suffered from serious damage, and the totally 5300 m long sections of the right side dike in the marsh, was also damaged during the earthquake.

According to the field reconnaissance report carried out after the earthquake, settlement of the dike due to the compression of the peat layer had reached about 2.4 m before the earthquake (Oshiki and Sasaki, 2001). And it was revealed elsewhere (Sasaki et al., 1993) that the cause of such a serious deformation of the dike was brought by the liquefaction in the bottom part of the embankment which settled down beneath the groundwater level.

Table 1. Kushiro-Oki Earthquake.

Date	15th Jan, 1993
Magnitude	M_j=7.8
Epicenter	N42º51' E114º23'
Depth	107 km
Maximum PGA	922gal

According to the report of damage for the Kushiro River dike by Hokkaido Development Bureau (1994), the lengths of the seriously failed sections were about 120-230 m each and they appeared periodically along the dike axis. The interval distances between these damaged parts were also 260-340 m each.

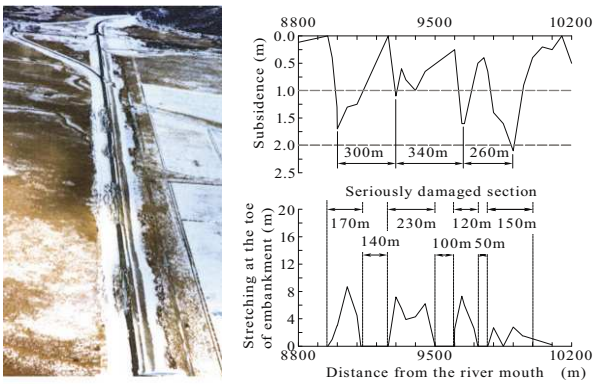

Figure 1. Aerial photograph of the Kushiro River dike and the distribution of the settlement and the stretching at the toe of the embankment.

Limited numbers of studies are carried out on this kind of phenomenon.

Hatanaka (1952) derived an equation of three dimensional response of an embankment and conducted shaking table tests to verify this equation. And he found that amplitude was larger at the locally limited spot along its longitudinal axis during the shaking. The phenomenon looked like a wave. However he concluded the response of the earth structure could be treated as the two dimensional problem when its length was long enough comparing to its height. He also conducted an experimental study on in-site measurement of seismic response of a groin (Hatanaka,1957).

Asada and Kawakami (1974) pointed out about the periodical appearance of failed sections to the Hachiro-gata dike during the Ogahanto-Oki Earthquake in 1964, to the run way of Niigata airport and Echigo Line of Japan National Railway during the Niigata Earthquake in 1964. And they concluded that the

Rayliegh wave was the cause of the periodical failure to these earth structures.

Ohmachi and Tokimatsu (1983) studied analytically and experimentally on the seismic response of a fill dam. They found that it was necessary to consider the three dimensional response on fill dam when the length of fill dams is in the range from two times to six times longer than its height.

As the cause of aforementioned periodical failure to the Kushiro dike is not clear, authors conducted a series of model tests on a shaking table to clarify the three dimensional behavior of an embankment during excitation (Hata et. al., 2003).

2 SHAKING TABLE TESTS

An electromagnetic shaking table (510 x 510 mm) was used. In this test, peak to peak amplitude of sinusoidal wave was set to be 1.0 mm for input motion. A frequency of the input wave was increased from 3 Hz to 35 Hz by step-by-step-wise. A model embankment was shaken to the perpendicular direction against the embankment axis.

Model embankments were simplified to have the cross sectional shape of a triangular like prism. Standard model embankment was 480 mm in length and 40 mm in height. A ratio of its height and width at bottom was 1:2. End boundaries of all the model embankments could slide on an end plate.

Model embankments were made from gelatin. Their shear modulus were from 1.04 to 6.71kPa, and the logarithmic decrement were about 10~15 %.

Table 2 shows the test condition of each test. A model embankment was placed on the shaking table directly in Case 1-1~1-5. In Case 1-1~1-5, the shear modulus of model embankment was varied as shown in Table 2. In Case 2-1~2-4, it was intended to simulate the condition of the embankment situated on the soft ground. The foundation ground was also made from gelatin, and the thickness of foundation ground was varied from 20 mm to 80 mm. Its length was 450 mm.

Target points for tracing the dynamic displacement were marked 10 mm intervals at the crest for all the model embankments as shown in Figure 2. The movements of these points were monitored by a CCD camera. After the shaking tests, the displacements of the target points were traced by an image analysis system. The recorded area was limited to 130 mm (lateral length) x 90 mm (vertical length) near the center of the model.

Figure 2. Photograph during the shaking.

As shown in Figure 2, the dynamic response of the model embankment was found to be periodically larger partly though the model base was shaken uniformly. The largely shaken parts of the crest do not move along the embankment axis during shaking if an input frequency is kept to be the same.

The waveform was obtained by fitting a sinusoidal curve to the observed displacement distribution of each target. It should be noted that because the recorded area was limited to 130 mm (lateral length), sinusoidal curve fitting could not be conducted correctly when the half wavelength was longer than 130 mm since the radius of curvature became too long.

The fitted curve to the displacement distribution of the crest is shown schematically in Figure 3. As shown in Figure 3, Y is defined as a longitudinal axis of the embankment and X is defined as the orthogonal axis perpendicular to the model axis. $X_{\max}$ and $X_{\min}$ are the extreme values of amplitude of wave. The amplitude at the anti-nodal point $X_{Antinode}$ is determined as the greater absolute value among $X_{\max}$ and $X_{\min}$. The amplitude at a nodal point, X_{Node} is determined as the amplitude at the halfway point between $X_{\max}$ and $X_{\min}$. So half–amplitude of the harmonic wave is obtained from the deference between them as ($X_{Antinode} - X_{Node}$). The sinusoidal wavelength l was determined from the fitted curve.

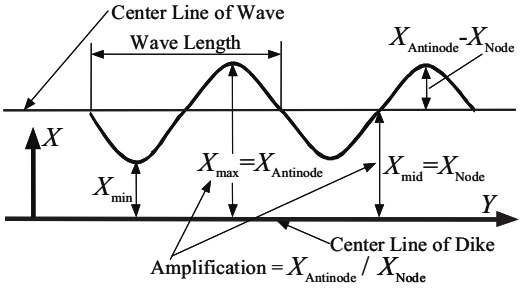

Figure 3. Definition of wave at the crest.

3 RESULTS OF SHAKING TABLE TESTS

Figure 4 shows the relationships between the frequency of shaking and the amplitude at the anti-nodal point, $X_{Antinode}$ in Case 1-1 ~1-5. Figure 5 shows the relationships between the frequency and the amplitude at nodal point. It is known from these figures that when $X_{Antinode}$ becomes the first peak, X_{Node} also becomes large. This means that the neutral axis of the waveform is also periodically displaced.

Figure 6 shows a ratio of amplitude at the anti-nodal point and at the nodal point in Case 1-1~1-5. From this figure, it is known that the ratio seems to be in the range from 1.1 to 1.6 under the condition of this experiment.

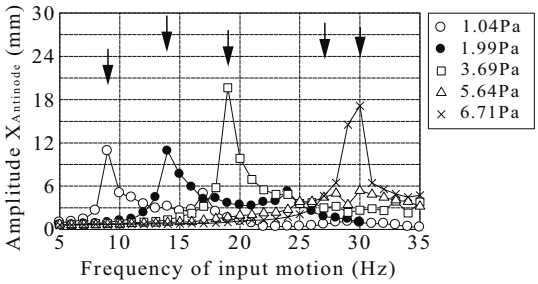

Figure 4. Amplitude at the anti-nodal point in Case 1-1~1-5.

Table 2. Condition of shaking table tests.

Case No	H (mm)	B (mm)	H:B/2	L (mm)	Shear modulus (kPa)	Thickness of soft ground (mm)
Case 1-1	39.8	83.0	1:1.04	480	1.04	0
Case 1-2	39.7	78.3	1:0.99	480	1.99	0
Case 1-3	41.0	82.4	1:1.01	480	3.69	0
Case 1-4	41.0	87.3	1:1.06	480	5.64	0
Case 1-5	41.0	84.7	1:1.03	480	6.71	0
Case 2-1	40.5	79.6	1:0.98	450	1.99	21.6
Case 2-2	39.8	80.5	1:1.01	450	1.99	38.8
Case 2-3	38.8	81.0	1:1.04	450	1.99	57.8
Case 2-4	37.7	79.3	1:1.05	450	1.99	79.8

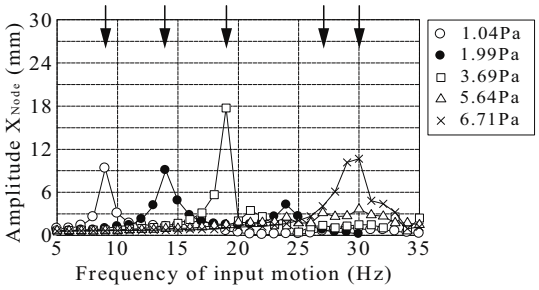

Figure 5. Amplitude at the nodal point in Case 1-1~1-5.

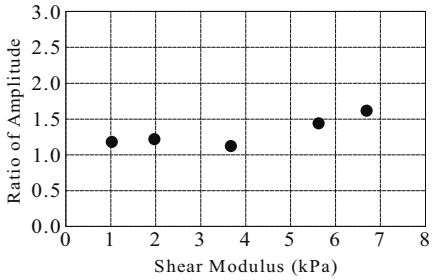

Figure 6. Ratio of amplitude between at the anti-nodal point and at the nodal point.

Figure 7 shows relationships between the frequency of input motion and the ratio of the wavelength and the height of model embankment, l/H in Case1-1~1-5. From this figure, it is known that the wavelength becomes longer when the model stiffness increases, though data points scattered due to the limitation of curve fitting at the high frequency range. Curves in this figure will be explained later.

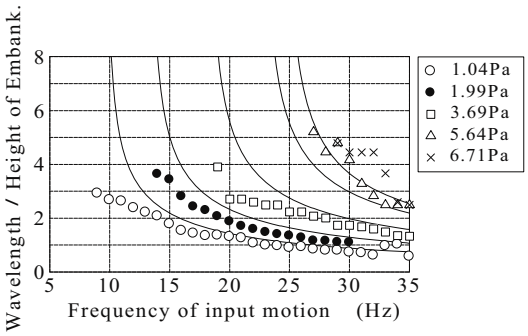

Figure 7. Relationship between the frequency of vibration and the ratio l/H in Case 1-1~1-5.

From the results of these tests, it was shown that the response of an embankment during shaking is not simply two dimensional in a cross sectional plane, but there appears a harmonic wave-like displacement distribution along the embankment axis. The wavelength and the amplitude of this wave vary with the change of the shear rigidity of the embankment and the frequency of the input motion.

Figure 8 shows a relationship between the wavelength at the crest of the embankment which lies on the soft ground and the frequency of the input motion in Case 2-1~2-4 and Case1-2. In this figure, the ratio of the wavelength is calculated against total height of embankments including the thickness of the ground. From this figure, it is known that the ratio of the wavelength becomes shorter as the thickness of soft ground increases.

Figure 9 shows amplitude at the toe of the embankment which lies on the soft ground. It is found that the amplitude at the anti-nodal point at the toe becomes larger than the one at the nodal point due to the three dimensional response of the embankment. This amplification of the ground motion is important in the case that the ground motion is marginally to cause the liquefaction. Therefore it is necessary to consider the effects of the three dimensional response on the amplification of ground surface to estimate the damage by liquefaction.

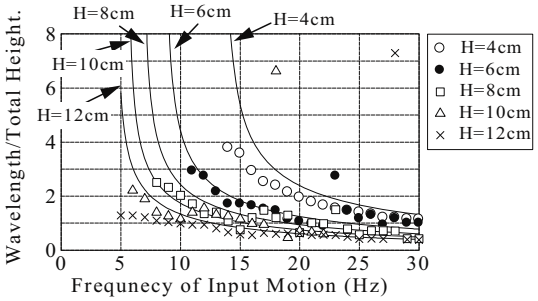

Figure 8. The relationship between the wavelength at the crest of the dike on the soft ground and the frequency of input motion.

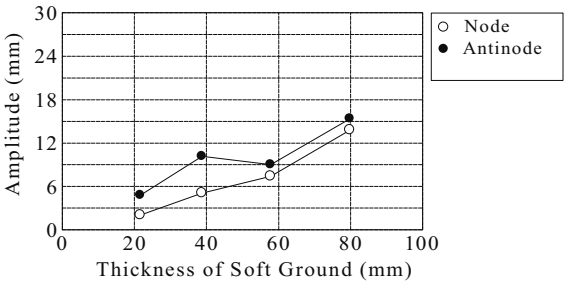

Figure 9. Amplitude at the toe of the embankment in Case 2-1~ 2-4.

4 DISCUSSION ON THE TEST RESULTS

Ohmachi and Tokimatsu (1983) reported about a three dimensional behavior of fill dams during an earthquake. They derived a following shear equation for seismic response of dam:

$$\rho \frac{\partial^2 u}{\partial t^2} = \left[\frac{1}{z} G(z) \left(\frac{\partial u}{\partial z} \right) + \frac{\partial}{\partial z} \left(G(z) \frac{\partial u}{\partial z} \right) + \frac{\partial}{\partial y} \left(G(z) \frac{\partial u}{\partial y} \right) \right] \tag{1}$$

where G is a function of z $\left(G(z) = G_0 z^a\right)$. This is same to the equation derived by Hatanaka for case of without damping. From Eq. (1), u can be considered as follows:

$$u(y,z,t) = Y(y) \cdot Z(z) \cdot e^{i\omega t} \tag{2}$$

where ω is a natural angular frequency. By substituting the Eq.(2) into Eq. (1), the following equations are derived:

$$Y_u(y) Z_u''(z) + \frac{1}{z} Y_u(y) Z_u'(z) + \frac{a}{z} Y_u(y) Z_u'(z) + Y_u''(y) Z_u(z) + \frac{\rho \omega^2}{G_0 z^a} Y_u(y) Z_u(z) = 0 \tag{3}$$

From Eq. (3) , Y and Z are derived as follows.

$$Y''(y) + \alpha^2 Y(y) = 0 \tag{4}$$

$$Z_u''(z) + \frac{1+a}{z} Z_u'(z) + \sqrt{\frac{\rho \omega^2}{G_0 z^a} - \alpha^2}\, Z_u(z) = 0 \tag{5}$$

Solution for Eq. (4) is given as follows:

$$Y = A \cdot \sin \alpha y \tag{6}$$

where A is constant, $\alpha = 2n\pi / l$, l is the wavelength in Y direction.

Solution for Eq. (5) is given as follows when $a = 0$, where the rigidity of the embankment material is constant:

$$Z(z) = cJ_0(\lambda z) \tag{7}$$

where c is constant, J_0 is the 0th Bessel function, $\lambda = \sqrt{\rho\omega^2/G_0 - \alpha^2}$.

When $z = H$, $Z(H) = 0$. H is the height of the embankment. From $Z(H) = cJ_0(\lambda H) = 0$, $\lambda H = \mu_m$ should be satisfied. μ_m is the value of m th-degree which satisfies Bessel function $J_0(\mu_m) = 0$ and m means the degree of mode of deformation for the vertical direction. Therefore the next equation is obtained.

$$\sqrt{\frac{\rho\omega^2}{G_0} - \left(\frac{2n\pi}{l}\right)^2} \times H = \mu_m \quad \Leftrightarrow l = \frac{2n\pi}{\sqrt{\frac{\rho\omega^2}{G_0} - \frac{\mu_m^2}{H^2}}} \tag{8}$$

From Eq.(8), the relationship between the natural frequency of the embankment f_{mn} and μ_m is obtained as follows by substituting $\omega = 2\pi f$ and $V_s^2 = G_0/\rho$:

$$f_{mn} = \frac{V_s}{2\pi H}\sqrt{\frac{4n^2\pi^2H^2}{l^2} + \mu_m^2} \tag{9}$$

where V_s is the shear wave velocity of the embankment. When the mode of deformation is $m = n = 1$, the equation which shows the relationship between the wavelength l and f_{11} , H , V_s is as follows.

$$l = \frac{2\pi H V_s}{\sqrt{4\pi^2 f_{11}^2 H^2 - \mu_1^2 V_s^2}} \quad (\mu_1 = 2.4048) \tag{10}$$

As l , the wavelength, is real number, the denominator of right side of Eq. (10) must be a rational number. Hence, Eq. (11) should be satisfied.

$$4H^2\pi^2 f_{11}^2 - \mu_1^2 V_s^2 \geq 0 \tag{11}$$

A natural frequency of embankment during shearing vibration can be calculated by $f_s = V_s/4H$, and substituting this equation into Eq. (11), the next inequality is obtained.

$$f_{11} \geq 1.53 f_s \tag{12}$$

A natural frequency of an embankment which has triangular cross sectional shape is almost 1.53 times higher than f_s . So the wave at the crest appears when the predominant frequency of input motion is higher than its natural frequency.

Calculated curves from Eq. (10) are shown in Fig.7 and 8. In the case with soft ground, the total height is used. From these figure, the calculated curves are in good agreement with the results of shaking table tests.

In the case of multi-layer systems where shear velocity is different form each others, the mean shear wave velocity of multi-layered system can be used for Eq.(10), which is calculated from the following equation:

$$\overline{V_s} = \sum V_{si} \times H_i \Big/ \sum H_i \tag{13}$$

where H_i and V_{si} means the height and shear velocity at the i layer.

As mentioned before, the Kushiro River dike lies on the soft ground composed of peat layer, loose sand layer and clay layer. Total thickness of the foundation ground plus the dike height was about 14 m. The averaged shear wave velocity given by Eq. (13) is calculated in the range from 110 to 135 m/s.

Although the strong motion near the Kushiro River dike was not recorded during the 1993 Kushiro-Oki Earthquake, however the strong motion near the site was estimated from the record obtained at the Kushiro meteorological observatory (Finn et al., 1997). The natural period of the estimated strong motion is about 0.28 seconds.

Frequencies calculated from Eq. (10) for an interval of damaged sections becomes 300 m are shown in Figure 10. From this figure, f_{11} is almost 3 Hz. Then the natural periods is close to the natural period of input strong motion. Therefore it can be said that the actual damage location is in good agreement with the theoretical solutions.

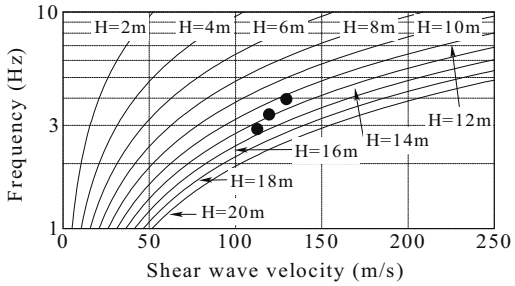

Figure 10. Frequency calculated from Eq.(10) in the case that an interval becomes 300 m .

5 CONCLUSIONS

This study aims to clarify effects on local failures of dikes during earthquakes. Conclusions obtained from this study are follows.

The displacement at the crest of embankment becomes larger at the locally limited spot even though model base was shaken uniformly.

And the reason why amplitude at the anti-nodal point becomes larger is due to the three dimensional response of embankment and the intervals between the damaged section can be calculated by Eq.(10).

REFERENCES

Asada, A. and Kawakami, F. 1975. Consideration on the characteristics of seismic motion in the grounds, *Journal of Journal of J. S.C.E.,* Vol.236, pp.93-107 (In Japanese)

Finn, W. D. L., Sasaki Y. and Wu G. 1997. Simulation of response of the Kushiro River dike to the 1993 Kushiro-Oki and 1994 Hokkaido Toho-Oki earthquakes, *Proceedings of the 14th ICSMGE,* Vol. 1, pp.99-102.

Hata Y., Kano. S. and Sasaki Y. 2003, Shaking table tests on 3-dimensional response during an earthquake, *JSCE Journal of Earthquake Engineering*, Paper No.251 (In Japanese).

Hatanaka M. 1952. Three dimensional consideration on the vibration of earth dams –on the free vibration-, *Civil Engineering*, Vol.37, No.10, pp.1-6 (In Japanese).

Hatanaka M. 1957. A few studies on the seismic response of groins, *Journal of J. S.C.E,*. Vol.44, pp.38-48 (in Japanese).

Hokkaido Development Bureau 1994. *Report of the restoration of the damaged dike due to the Kushiro-Oki Earthquake*, No.1 (In Japanese).

Ohmachi, T. and Tokimatsu, K. 1983. Formulation of a practical method for three dimensional earthquake response analysis of embankment dams, *Journal of J. S.C.E.,* No. 333, pp. 71-80 (In Japanese).

Oshiki H. and Sasaki Y.,2001. Restoration works of seismically damaged river dikes using remedial treatment of liquefiable layer, *Journal of Construction Management and Engineerin*g, No.686/VI-52, pp.15-29.

Sasaki, Y., Oshiki, H. and Nishikawa, J. 1993. Embankment failure caused by the Kushiro-Oki Earthquake of January 15, 1993, *the !3th I.C. S. M. F. E, Performance of Ground and Soil Structureuring Earthquakes*:, pp. 61-68.